



1 Sources of volatile organic compounds and policy implications for 2 regional ozone pollution control in an urban location of Nanjing, 3 East China

4 Qiuyue Zhao^{1,2}, Jun Bi^{1*}, Zhenghao Ling³, Qian Liu^{2*}, Guofeng Shen⁴, Feng Chen², Yuezhen Qiao²,
5 Chunyan Li², Zongwei Ma¹

6 ¹State Key Laboratory of Pollution Control and Resource Reuse, School of the Environment, Nanjing University,
7 Nanjing 210023, China

8 ²Jiangsu Key Laboratory of Environmental Engineering, Jiangsu Academy of Environmental Sciences, Nanjing
9 210036, China

10 ³School of Atmospheric Sciences, Sun Yat-sen University, Guangzhou 510275, China

11 ⁴College of Urban and Environmental Sciences, Peking University, Beijing 100871, China

12 *Correspondence to:* Jun Bi (jbi@nju.edu.cn) and Qian Liu (candyvz@msn.com)

13

14 **Abstract.** Understanding the composition, temporal variability, and source apportionment of volatile organic
15 compounds (VOCs) is necessary for determining effective control measures to minimize VOCs and its related
16 photochemical pollution. To provide a comprehensive analysis of VOC sources and their contributions to ozone
17 (O₃) formation in the Yangtze River Delta (YRD) - a region experiencing highest rates of industrial and economic
18 development in China, we conducted a one-year sampling exercise for the first time at an urban site in Nanjing
19 (JAES site). Alkanes were the dominant group at the JAES site, contributing ~53% to the observed total VOCs,
20 followed by aromatics (~17%), acetylene (~17%), and alkenes (~13%). We identified seasonal variability in
21 TVOCs with maximum and minimum concentrations in winter and summer, respectively. A morning and
22 evening peak and a daytime trough were identified in the diurnal VOCs patterns. We identified the source
23 apportionments of VOCs and their contributions to photochemical O₃ formation using the Positive Matrix
24 Factorization (PMF) and observation-based model together with a Master Chemical Mechanism (OBM-MCM).
25 The PMF model identified five dominant VOC sources, with highest contributions from diesel vehicular
26 exhausts (34 ± 5%), followed by gasoline vehicular exhausts (27 ± 3%), industrial emissions (19 ± 2%), fuel
27 evaporation (15 ± 2%) and biogenic emissions (4 ± 1%). The results from the OBM-MCM model simulation
28 inferred photochemical O₃ formation to be VOC-limited at the JAES site when considering both the reactivity
29 and abundance of the individual VOC species in each source category. Further, VOCs from vehicular and
30 industrial emissions were found to be the dominant control on O₃ formation, particularly the VOC species *m,p*-
31 xylene, toluene and propene, which top priorities should be given to the alleviation of photochemical smog.
32 However, when considering the reactivity and abundance of VOC species, the contribution of biogenic emissions
33 to O₃ pollution was significantly reduced. Our results therefore highlight the need to consider both the abundance
34 and reactivity of individual VOC species in order to develop effective control strategies to minimize
35 photochemical pollution in Nanjing.

36 1. Introduction

37 Volatile organic compounds (VOCs) are key precursors of O₃ and secondary organic aerosols (SOA) - a major
38 component of fine particulate matter (PM_{2.5}). VOCs significantly contribute to the formation of photochemical
39 smog, atmospheric oxidative capacity, visibility degradation, and global climate (Jenkin and Clemmshaw, 2000;
40 Seinfeld and Pandis, 2006), and some VOCs are also known to be toxic to human health. Therefore, in recent
41 years, much research has focused on the impacts of VOCs due to their influence on atmospheric chemistry and
42 impacts on human health (Shao et al., 2009 and references therein).

43

44 The Yangtze River Delta (YRD) region (Shanghai-Jiangsu-Zhenjiang region) is one of the fastest growing
45 regions in China, having recently undergone rapid urbanization and industrialization. Rapid economic growth



46 has been associated with increased photochemical smog and elevated concentrations of ground-level O₃ and fine
47 particulate matter (PM_{2.5}). These conditions have been listed as the most important sources of pollution affecting
48 the population in the YRD region, and are likely caused by increasing concentrations of VOCs. Therefore, it has
49 been suggested that controlling VOC emissions is necessary for the effective alleviation of photochemical smog
50 (Wang et al., 2009; Zhang et al., 2009; Cai et al., 2010; Kurokawa et al., 2013; Ding et al., 2016).

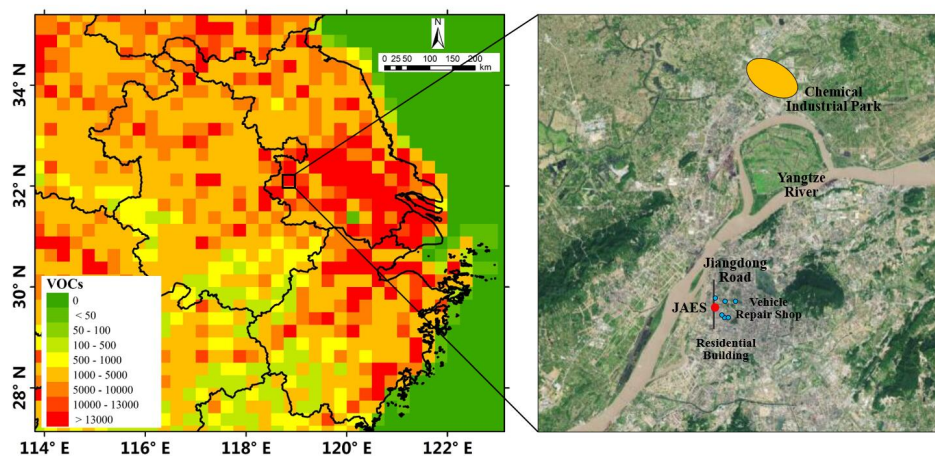
51
52 To further understand VOC characteristics and to develop effective policies towards lowering VOC emissions,
53 a number of sampling campaigns have been conducted to investigate the components, mixing ratios,
54 photochemical reactivity and emissions of VOCs over the YRD region (Mo et al., 2015; Pan et al., 2015; An et
55 al., 2014; Cai et al., 2010; Shao et al., 2016; Xu et al., 2017). For example, based on continuous observation data
56 collected from March, 2011 to February, 2012, An et al. (2014) identified clear seasonal VOCs variability in an
57 industrial area of Nanjing, with maximum and minimum levels observed in summer and winter, respectively.
58 VOC variability was also found to be strongly influenced by industrial emissions. In contrast, Mo et al. (2017)
59 found no difference in VOC chemical compositions between residential, industrial and suburban areas of the
60 coastal industrial city, Ningbo. By comparing the emission-based profiles and those extracted from the positive
61 matrix factorization (PMF) model, the photochemical industry was identified as the highest contributor of
62 ambient VOCs due to the unique industrial structure of Ningbo (Mo et al., 2015, 2016). Pan et al. (2015)
63 conducted emissions measurements of open biomass burning in the rural area of the YRD region and examined
64 the major contributors to O₃ pollution using a box model together with the Regional Atmospheric Chemical
65 Mechanism. Overall, these studies were conducted in industrialized and/or rural areas of the YRD region and
66 demonstrated the contributions of industrial emissions and biomass burning towards ambient VOC levels and
67 their contributions to O₃ formation. However, VOC studies in urban areas of the YRD region are limited and
68 could help to improve our understanding of the spatial variability of VOCs and their environmental impact,
69 particularly as stricter policies on VOCs and/or photochemical smog have been implemented since 2013 (Fu et
70 al., 2016). Furthermore, the sampling resolution and sampling duration of these studies were relatively low as
71 the samples were collected using canisters. High-resolution VOC datasets can provide more detailed information
72 on the temporal and spatial variability, source apportionments, and impact factors of VOCs.

73
74 In this study, we collected continuous one-year observational VOC data at an urban site in Nanjing in the YRD
75 region. The seasonal and diurnal characteristics of VOCs were investigated, and their sources were identified
76 and quantified using the PMF model. Furthermore, we used a box model together with a Master Chemical
77 Mechanism (OBM-MCM) to identify the O₃-precursor relationships and the contributions of VOC sources to
78 photochemical O₃ formation. Our results were compared with VOCs data from other Chinese megacities. Based
79 on these findings, we summarized and proposed control strategies to minimize VOCs pollution and assessed
80 their implications for Nanjing and the wider YRD region. The results provide useful information towards
81 lowering photochemical pollution in the YRD region as well as other regions in China.

82 **2. Methodology**

83 **2.1. Sampling campaign**

84 We continuously measured VOC concentrations from January to December, 2016, at an observation station on
85 the rooftop of an office building (~80 m above the ground level) of the Jiangsu Academy of Environmental
86 Science (JAES). The station is located in an urban area of Nanjing, and is surrounded by heavy road traffic,
87 residential buildings, a plant and flower market, and several auto repair shops (Fig. 1). Nanjing, located in the
88 western part of the YRD region, is one of the most urbanized and industrialized areas in the world and
89 consequently experiences severe air pollution. The site is located downwind of both Nanjing city center and the
90 wider YRD region (Zhao et al., 2017; Zhou et al., 2017), and is therefore ideally placed to determine the
91 combined impacts of VOCs from both local and regional atmospheric pollution.



92
93 **Figure 1. (a) Maps of the study location showing VOCs emission at a resolution of 0.25 degrees (MG/a) (The data were from**
94 **MEIC emission inventory (www.meicmodel.org, last access date:15 September 2019)). (b) The location of the JAES**
95 **sampling site is indicated by a red circle (The base map was from © Baidu Maps). The blue circles indicate vehicle repair**
96 **shops, the yellow circle indicates chemical industry park and the black solid line indicates a heavy traffic road**

97 Fifty-six VOC species including alkanes, alkenes, aromatics, and acetylene were measured at 1-h intervals using
98 a PerkinElmer Online Ozone Precursor Analyzer based on a thermal desorption-GC system. First, the dried air
99 samples were collected by a thermal desorption instrument and subsequently pre-concentrated onto a cold trap.
100 The sampling flow was 15 mL/min. The sample was enriched after 600 mL of air sample, and the cold trap was
101 heated to resolve the compounds adsorbed on it. By applying the Dean's Switch technology, the low- and high-
102 volatile components were injected into the $\text{Al}_2\text{O}_3/\text{Na}_2\text{SO}_4$ PLOT column ($50\text{ m} \times 0.22\text{ mm} \times 1\text{ }\mu\text{m}$) and the
103 dimethyl siloxane column ($50\text{ m} \times 0.32\text{ mm} \times 1\text{ }\mu\text{m}$), respectively, and analyzed using a flame ionization detector
104 (FID). The temperature increased from 46 °C for 15 min to 170 °C at a rate of 5 °C/min, and then to 200 °C at
105 a rate of 15 °C/min. The samples were finally held at 200 °C for 6 min.

106
107 A calibration was performed daily for quality control. The calibration curves showed good linearity with a
108 correlation coefficient of 0.99. Seven repeated analyses were performed to test the precision of the 56 species
109 using a gas standard mixture with species concentrations ranging from 20 to 49 ppbC. The relative standard
110 deviations of most of the 56 species were < 5%, representing an error of < 0.5 ppbC.

111 2.2. The PMF model for VOC source identification

112 In this study, the PMF (version 4.0) model was applied to the observed VOC data to identify potential VOC
113 sources. A detailed description of the PMF model is provided by Yuan et al. (2009) and Ling et al. (2011). In
114 brief, the PMF model is a receptor model, which can identify the sources and contributions of given species
115 without prior input of their source profiles. In this study, a total of 25 species were selected as the input for the
116 PMF model including species with high abundances as well as typical tracers of emission sources. Species with
117 high percentages of missing values (> 25%) were excluded (*i.e.*, 1,3-butadiene, cis/trans-2-pentene,
118 dimethylpentane, and trimethylpentane). The total concentration of the 25 selected species accounted for ~92%
119 of the total measured VOC composition. Furthermore, we calculated the total reactivity of the selected 25 species
120 to be ~90% of the total measured VOCs by combining the VOC concentrations and OH radical loss rates (L_{OH})
121 (Shao et al., 2009). The high abundance and total reactivity contributions suggests that the selected 25 species
122 were appropriate for the PMF model simulation.

123
124 The PMF model was tested with a variety of factors, and the optimum source profiles and contributions were
125 determined based on the correlation between modelled and observed data, the comparison of modelled profiles
126 with the results from emission-based measurements, and other PMF model simulations (*i.e.*, HKEPD, 2015;



127 Wang et al., 2014; An et al., 2014; Liu et al., 2008a).

128 2.3. VOC contributions on O₃ formation using the observation-based model

129 In this study, we applied the observation-based model (OBM) coupled with the MCM (version 3.2), which
130 consists of ~6000 reactions involving ~16,500 species without considering vertical and horizontal transport, to
131 quantify the contributions of VOC emission sources to photochemical O₃ formation. This model has been widely
132 used to identify the photochemical reactivity and photochemical products in different environments (Volkamer
133 et al., 2007; Xue et al., 2014; Li et al., 2014; He et al., 2019). Detailed configurations of the model have been
134 introduced in previous studies (Saunders et al., 2003; Lam et al., 2013). In this study, the hourly data of VOCs,
135 trace gases (i.e., CO, NO_x, SO₂, and O₃), and meteorological parameters on 88 O₃ episode days (identified as
136 hourly maximum O₃ concentrations > 80 ppbv per day) were used as the input for the model. To simulate each
137 O₃ episode day, we ran the model for two-days using the mean diurnal variability of the input species during the
138 whole sampling period to achieve a steady state for the unmeasured mixing ratios of species with a short lifetime,
139 i.e., OH and HO₂ radicals (Wang et al., 2017; Sun et al., 2018).

140
141 To simulate O₃ formation, we used the model to calculate the relative incremental reactivity (RIR) to assess the
142 sensitivity of O₃ photochemical formation to changes in the concentrations of its precursors (Carter and Atkinson,
143 1989; Cardelino and Chameides, 1995). The RIR is defined as the percent change in O₃ production per percent
144 change in precursors and is calculated as shown in Eq. (1), while the average RIR of precursor *X* is calculated as
145 shown in Eq. (2).

$$146 \quad RIR^S(X) = \frac{P_{O_3-NO}^S(X) - P_{O_3-NO}^S(X-\Delta X)}{\Delta S(X)/S(X)} / P_{O_3-NO}^S(X) \quad (1)$$

$$147 \quad \overline{RIR} = \frac{\sum_1^N [RIR^S(X) P_{O_3-NO}^S(X)]}{\sum_1^N P_{O_3-NO}^S(X)} \quad (2)$$

148 where the superscript *S* is the specific sample day; *S*(*X*) represents the measured concentration of precursor *X*,
149 including the amounts emitted at the site and those transported to the site; $\Delta S(X)$ is a hypothetical change in the
150 concentration of precursor *X* (10% *S*(*X*) in this study); and *N* is the number of evaluated days. $P_{O_3-NO}^S$ is the O₃
151 formation potential, which is the net O₃ production and NO consumed during the evaluation period.

152 Furthermore, to investigate the relative importance of the precursor species to photochemical O₃ formation, the
153 RIR-weighted values and the relative contributions of different precursors were calculated as shown in Eq. (3)
154 and Eq. (4), taking into consideration both the reactivity and abundance of VOC species (Ling et al., 2011; Ling
155 and Guo, 2014).

$$156 \quad RIR\text{-weighted}(X) = \overline{RIR}^X \times conc(X) \quad (3)$$

$$157 \quad Contribution(X) = \frac{\overline{RIR}^X \times conc(X)}{\sum [\overline{RIR}^X \times conc(X)]} \quad (4)$$

158 where *X* represents the specific precursor, \overline{RIR}^X is the average RIR value of precursor *X*, and *conc*(*X*) is the
159 concentration of precursor *X*.

160 3. Results and discussion

161 3.1 VOCs observation statistics

162 Table 1 shows the average concentration and standard deviation of fifty-six VOC species concentrations
163 measured at the JAES site. The annual average total VOC (TVOC) concentrations in 2016 was 25.7 ± 19.1 ppbv,
164 with highest contributions from alkanes (13.6 ± 10.5 ppbv, ~53%), followed by aromatics (4.4 ± 4.0 ppbv, ~17%),
165 acetylene (4.5 ± 5.5 ppbv, ~17%) and alkenes (3.2 ± 3.3 ppbv, ~13%). Annually, the most abundant 10 species
166 were acetylene, propane, ethane, ethylene, butane, toluene, *i*-pentane, *i*-butane, propylene and benzene, with a
167 combined contribution of ~77% of the TVOC. This observed VOC composition suggests that VOCs at the JAES
168 site are predominantly sourced from combustion emissions (i.e., vehicular emissions). Alkenes are mainly
169 associated with vehicular emissions and are more photochemically reactive relative to alkanes and aromatics.



170 The alkenes were found to have higher mixing ratios during weekdays relative to the weekends (2.9 ± 0.1 vs 3.5
 171 ± 0.2 ppbv for weekdays and weekend, respectively, $p < 0.05$), further confirming the dominant contribution of
 172 vehicular emissions to VOC levels at the JAES site.

173
 174 **Table 1. The average range and standard deviation of VOC species concentrations measured at the JAES site from January**
 175 **to December 2016.**

Species	Average \pm Standard deviation (ppbv)	Species	Average \pm Standard deviation (ppbv)
Alkanes	13.64 \pm 10.53	Alkenes	3.24 \pm 3.28
ethane	3.63 \pm 2.68	ethene	1.72 \pm 2.00
propane	3.70 \pm 3.01	propylene	0.92 \pm 1.16
<i>i</i> -butane	1.03 \pm 0.87	1-butene	0.12 \pm 0.16
<i>n</i> -butane	1.55 \pm 1.26	cis-2-butene	0.06 \pm 0.09
cyclopentane	0.08 \pm 0.10	trans-2-butene	0.16 \pm 0.11
<i>i</i> -pentane	1.15 \pm 1.24	1-pentene	0.03 \pm 0.03
<i>n</i> -pentane	0.61 \pm 0.60	cis-1-pentene	0.02 \pm 0.03
2,2-dimethylbutane	0.02 \pm 0.02	trans-2-pentene	0.02 \pm 0.03
2,3-dimethylbutane	0.05 \pm 0.07	isoprene	0.14 \pm 0.20
2-methylpentane	0.26 \pm 0.29	<i>n</i> -hexene	0.05 \pm 0.03
3-methylpentane	0.16 \pm 0.21	Aromatics	4.40 \pm 4.01
<i>n</i> -hexane	0.40 \pm 0.45	benzene	0.80 \pm 0.70
methylcyclopentane	0.26 \pm 0.27	toluene	1.40 \pm 1.35
cyclohexane	0.10 \pm 0.16	ethylbenzene	0.50 \pm 0.62
2,4-dimethylpentane	0.03 \pm 0.01	<i>m/p</i> -xylene	0.70 \pm 0.71
2,3-dimethylpentane	0.03 \pm 0.02	<i>o</i> -xylene	0.25 \pm 0.24
2-methylhexane	0.06 \pm 0.09	styrene	0.12 \pm 0.17
3-methylhexane	0.07 \pm 0.10	<i>n</i> -propylbenzene	0.03 \pm 0.03
heptane	0.09 \pm 0.11	<i>i</i> -propylbenzene	0.03 \pm 0.04
methylcyclohexane	0.07 \pm 0.09	<i>m</i> -ethyltoluene	0.11 \pm 0.14
2,2,4-trimethylpentane	0.02 \pm 0.03	<i>p</i> -ethyltoluene	0.05 \pm 0.07
2,3,4-trimethylpentane	0.02 \pm 0.01	<i>o</i> -ethyltoluene	0.04 \pm 0.05
2-methylheptane	0.02 \pm 0.02	1,3,5-trimethylbenzene	0.04 \pm 0.06
3-methylheptane	0.02 \pm 0.02	1,2,4-trimethylbenzene	0.15 \pm 0.21
octane	0.04 \pm 0.06	1,2,3-trimethylpentane	0.10 \pm 0.14
nonane	0.02 \pm 0.02	<i>m</i> -diethylbenzene	0.03 \pm 0.06
decane	0.04 \pm 0.04	<i>p</i> -diethylbenzene	0.04 \pm 0.08
undecane	0.04 \pm 0.07	Acetylene	4.47 \pm 5.49
dodecane	0.09 \pm 0.20	--	--

176

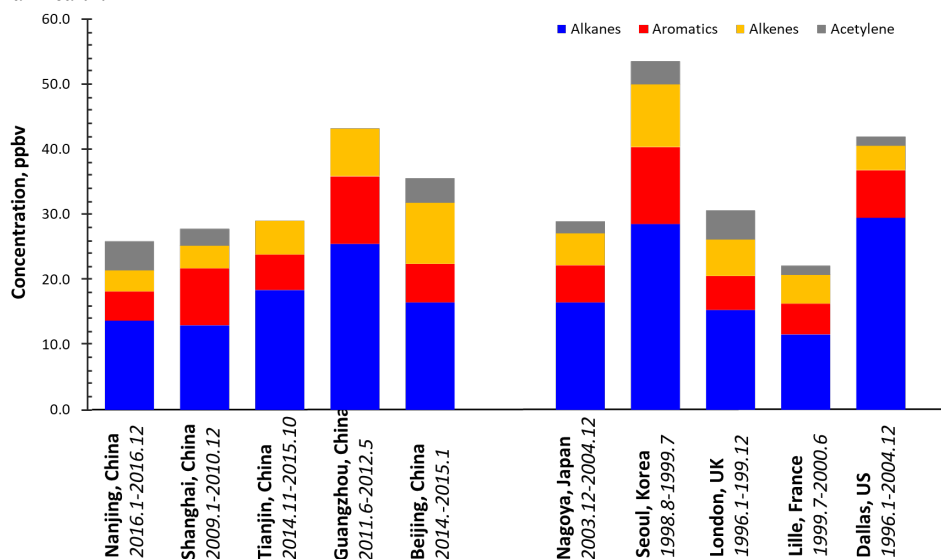
177

178 The TVOC level in this study was lower than previous measurements from an industrial site in Nanjing, in which
 179 43.5 ppbv TVOC was reported (An et al., 2014). However, the high TVOC levels are likely due to the proximity
 180 of the observation site (~ 3 km northeast) to the Nanjing chemical industry area, as well as several iron, steel, and
 181 cogeneration power plants (within 2 km) (An et al., 2014). The variability in land-use between these two studies
 182 have also resulted in distinct VOC component profiles. In the industrial area, the relative contributions of alkenes
 183 and aromatics were as high as 25% and 22%, while the contribution of alkynes was only 7% (An et al., 2014).



184 The alkane, alkene, and aromatic concentrations from the industrial site were 1.4, 3.4, and 2.2 times higher than
185 the concentrations of this study, respectively, while alkyne concentrations were ~30% lower. Given the large
186 variability observed between the two sites, it is crucial to assess the spatial variability of ambient VOCs across
187 the city through a collaboration of multiple research groups using available real-time and online VOC monitoring
188 systems.

189
190 Table S1 compares reported ambient VOCs from continuous measurements of ≥ 1 year in several megacities in
191 a number of countries, including China. Continuous online measurements of ambient VOCs have only been
192 available in China since 2010, unlike many developed countries whereby online VOC measurements have been
193 available since the year 2000. In China, such measurements are only concentrated in a few megacities, including
194 Beijing, Guangzhou, and Shanghai. The TVOC level reported in Nanjing was close to levels measured in
195 Shanghai (another megacity in the YRD, East China, 27.8 ppbv) (Wang et al., 2013), Tianjin (a megacity in
196 North China, 28.7 ppbv) (Liu et al., 2016), and Wuhan (a megacity located in central China, 24.3 ppbv) (Lyu et
197 al., 2016), but was considerably lower than Beijing (north China, 35.2 ppbv) (Zhang et al., 2017) and Guangzhou
198 (south China, 42.7 ppbv) (Zou et al., 2015). Alkanes were the dominant hydrocarbon group in all the cities;
199 however, some differences in relative contributions of the four classes were observed. The contribution from
200 aromatics was highest in Shanghai (31%) relative to the other cities, which is likely explained by the large
201 petrochemical and steel industry in Shanghai (Wang et al., 2013, Huang et al., 2011). In comparison, the
202 contribution of aromatics in Guangzhou (Zou et al., 2015) and the industrial area in Nanjing (An et al., 2014)
203 were 24% and 22%, respectively, while in other cities the contribution ranged between 17-19%. The current
204 ambient VOCs concentrations in Chinese megacities are generally comparable to the urban VOCs levels in
205 developed countries during the year 2000. Chinese megacities are therefore experiencing much higher ambient
206 VOCs contamination, given the remarkable decrease in VOC emissions in developed countries over the last two
207 decades (European Environment Agency, 2016; U.S. EPA, 2017; Pan et al., 2015). High VOCs levels in Chinese
208 megacities are known to impact ambient ozone and secondary particle pollution, as well as cause adverse impacts
209 on human health.



210
211 Figure 2. Comparison of annual average concentrations of ambient VOC in different cities based on real-time online
212 continuous measurements of at least one year.

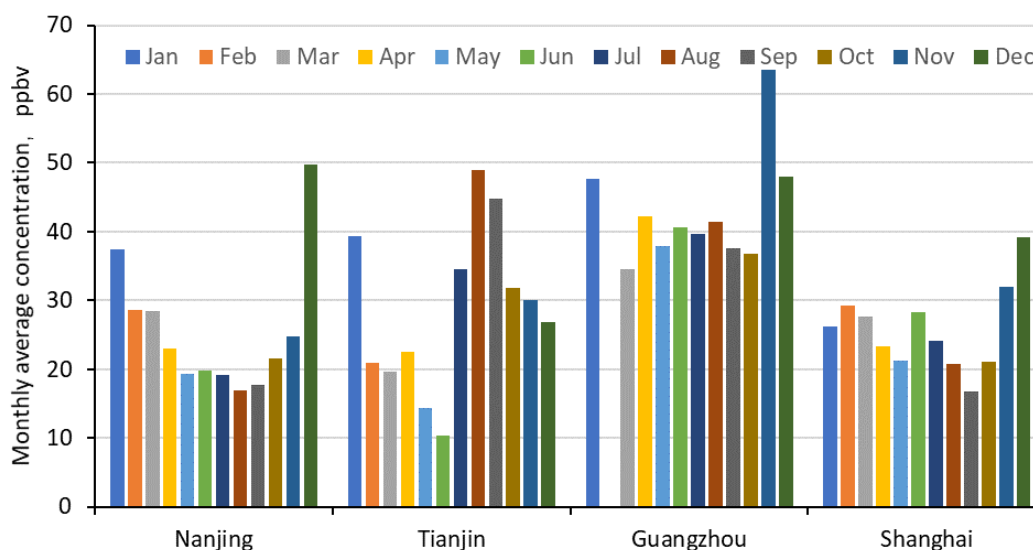
213 3.2 Temporal variability

214 In this study, ambient VOCs showed significant seasonal variability, with relatively high monthly average
215 concentrations in winter (40.2 ± 24.0 ppbv) and spring (23.8 ± 15.0 ppbv), and low concentrations in summer



216 (18.5 ± 14.6 ppbv) and autumn (20.1 ± 12.2 ppbv). As shown in Fig. S1, the highest monthly average
217 concentration was observed in December, followed by January. High pollution levels during the winter period
218 are usually expected and is explained by atmospheric temperature inversions caused by cooler weather, which
219 inhibits particle dispersion. Lower concentrations during the summer period are due to both favorable diffusion
220 conditions and photochemical degradation of VOCs.

221
222 High wintertime VOCs pollution were also reported in Shanghai (Wang et al., 2013), Guangzhou (Zou et al.,
223 2015), and Tianjin (Liu et al., 2016), though some differences in the monthly VOCs variability were also
224 observed. Except for the winter months, similar (and relatively stable) ambient VOCs levels in the remaining
225 months were observed for Guangdong (Fig. 3). In Shanghai, relatively high ambient VOCs were also observed
226 in June-July. The peak value in June can be explained by chemical and petrochemical industrial sites located
227 upwind of the monitoring site (Wang et al., 2013). VOCs concentrations in Tianjin showed significant monthly
228 variability. Highest concentrations were reported in autumn and lowest concentrations were reported in summer.
229 The observed monthly variability is affected by several factors including the type and level of emissions and
230 local meteorological conditions.



231
232 **Figure 3. Monthly variability of ambient VOCs at the JAES site and three other Chinese cities, Shanghai (Wang et al., 2013),**
233 **Guangzhou (Zou et al., 2015), and Tianjin (Liu et al., 2016).**

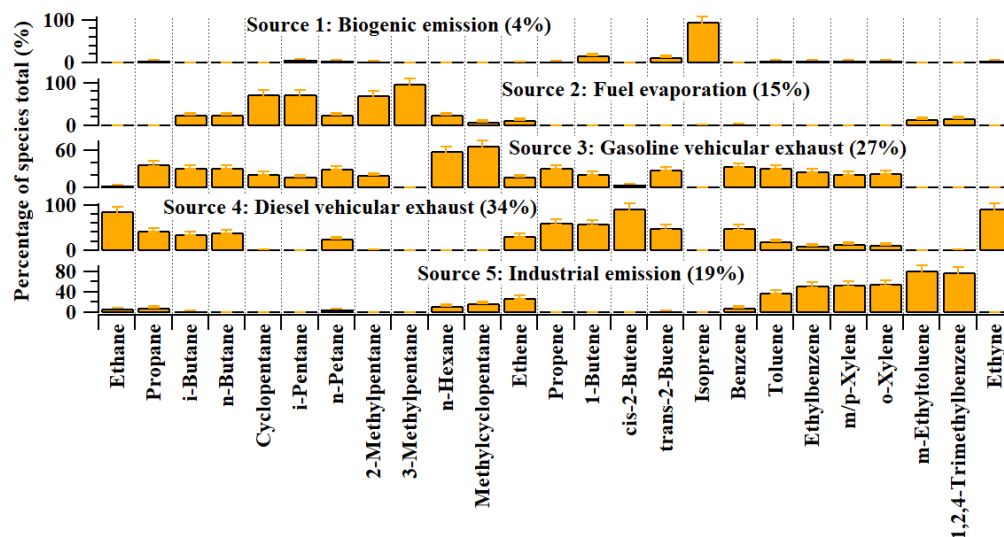
234 Figure S3 shows the diurnal trends in ambient VOCs for each month. The diurnal patterns were generally similar
235 for all the months. The observed peak at approximately 8-9 am (local time) corresponds with the city's morning
236 traffic rush. The concentration begins to decrease after 9 am, with lowest concentrations observed at
237 approximately 3 pm. The observed decline was likely due to reduced vehicle emissions, growth of the inversion
238 top, and enhanced photochemical VOC degradation. After 3 pm, the concentrations begin to increase gradually
239 as a result of increased vehicle emissions during the evening rush hour, as well as a reduction in the atmospheric
240 mixing height under evening meteorological conditions. The second evening VOCs peak was less prominent
241 than the morning peak. Evening concentrations were generally higher than the daytime concentrations, and the
242 amplitudes of diurnal variability were larger in autumn and summer compared to winter and spring.

243



244 3.3 Source apportionment of VOCs

245 In this study, we applied the PMF model to apportion the sources of VOCs at the sampling site. Figure 4
246 illustrates the source profiles of the VOCs produced by the PMF model. The model identified five VOCs sources,
247 including biogenic emissions (Source 1), fuel evaporation (Source 2), gasoline vehicular exhausts (Source 3),
248 diesel vehicular exhausts (Source 4), and industrial emissions (Source 5). Source 1 was identified as biogenic
249 emissions due to the high loading of isoprene – a typical tracer of biogenic emissions (Yuan et al., 2012; Lau et
250 al., 2010). Source 2 was represented by high proportions of 2-methylpentane, 3-methylpentane, *i*-pentane, and
251 cyclopentane. Pentanes are mainly associated with gasoline emissions. However, the low contributions of
252 incomplete combustion tracers in this profile suggests that the VOCs are sourced from fuel evaporation (An et
253 al., 2015); thus, Source 2 was identified as fuel evaporation. Source 3 and Source 4 were identified as vehicular
254 exhausts due to their high loadings of incomplete combustion tracers, i.e., C₂-C₄ alkanes and alkenes (Guo et al.,
255 2011a, b). Higher proportions of *n*/*i*-pentane, *n*-hexane, and methylcyclopentane in Source 3 relative to Source
256 4 indicates VOCs sourced from gasoline vehicular exhausts (Ling et al., 2011; Guo et al., 2011b; Liu et al.,
257 2008b). Source 4 was identified as diesel vehicular exhausts due to the high percentages of ethyne, ethane, and
258 propene, as well as C₂-C₄ alkenes (Ou et al., 2015; Liu et al., 2008c; Cai et al., 2010). Furthermore, high
259 concentrations of aromatics were identified in Source 5. Aromatics are frequently observed in the profiles of
260 solvents used in a variety of industries, including shoe making, paint, printing, and petroleum (Guo et al., 2016;
261 Lau et al., 2010; Yuan et al., 2009; Song et al., 2008). In addition, the profile of Source 5 was consistent with the
262 chemical profiles of the measured industrial emissions at the industrial site in Nanjing. Therefore, Source 5 was
263 identified as industrial emissions.



264
265 **Figure 4. Source profiles of VOCs identified using the PMF model and the relative contributions of the individual VOC**
266 **species.**

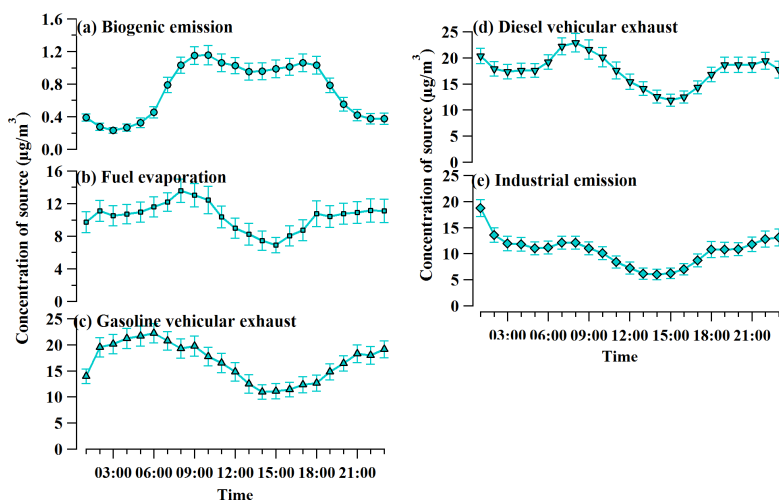
267
268 Vehicular exhausts were found to be the most significant contributor to the TVOCs at the JAES site, with average
269 contributions of ~34% and ~27% for diesel and gasoline exhausts, respectively, followed by industrial emissions
270 (19%), fuel evaporation (~15%), and biogenic emissions (~4%). Our results are in contrast to previous results
271 observed at industrial sites in Nanjing (An et al., 2014; Xia et al., 2014a). An et al. (2014) found that industrial
272 activities were the most significant source of VOCs, contributing 45%-63% (mainly aromatic VOCs), followed
273 by vehicle emission at 34%-50%. Similarly, Xia et al. (2014a) reported solvent usage and other industrial sources
274 to account for most (31%) of the VOCs in a suburban site in southwestern Nanjing, close in proximity to
275 Nanjing's industrial zone. Fossil fuel/biomass/biofuel combustion were the second highest contributors at 28%,



276 while the average contribution of vehicular emissions was 17%, mainly from the northern center of Nanjing (Xia
277 et al., 2014a). Combined, these results infer vehicular emissions to be a major component of urban emissions in
278 Nanjing. The observed spatial variability in the contributions of VOC sources infers the complex emissions
279 characteristics of VOCs in Nanjing, likely due to the city's unique industrial structure. These results also
280 demonstrate that local emissions are dominant contributors to ambient VOCs levels in Nanjing.

281
282 The dominant contribution of vehicular emissions to ambient VOCs in Nanjing is consistent with the
283 urban/central areas of other large cities, including Hong Kong, Guangzhou, Shanghai, and Beijing, as identified
284 and quantified by the PMF model (Guo et al., 2011a; Yuan et al., 2009; Wang et al., 2015; Zhang et al., 2013;
285 Cai et al., 2010). In addition, our results are in agreement with the anthropogenic VOC source emission inventory
286 of Jiangsu Province in 2010 (Xia et al., 2014b), indicating vehicular emissions and industrial emissions (i.e.,
287 solvent usage and industrial process source) to be the two dominant sources of VOCs in the region. However,
288 the contributions of vehicle related emissions (i.e., ~25%) and industrial emissions were lower and higher than
289 those quantified by the PMF model in this study, respectively. The observed discrepancy between the two studies
290 may be due to differences in source categories, measured VOC species, and/or sampling locations and methods
291 used in the different models. For example, the VOC sources in Jiangsu province were categorized into vehicular
292 related emission (~26%), industrial solvent usage (~25%), fossil fuel combustion (~24%), industrial processes
293 (~22%) and biomass burning (~3%). Further, vehicle related emissions only included emissions from motor
294 vehicles and ships, and the volatilization of fuel, while solvent usage included organic solvents volatilized from
295 a variety of industries (the industrial produce process of electronic equipment manufacturing, furniture
296 manufacturing, printing, packaging, inks, adhesives, etc. and other dry cleaning, catering, and architectural
297 decoration processes). Higher vehicular emission contribution in this study may also be due to the increasing
298 number of vehicles from 2010-2014 as a result of increased urbanization and industrialization (Statistical
299 yearbook of Nanjing, 2014).

300
301 Figure 5 illustrates the mean diurnal variability of all identified source at the JAES site. These trends were
302 influenced by the variability in emission strength, mixing height, and the concentrations and photochemical
303 reactivity of individual species in each source profile. For example, we observed a typical diurnal pattern with a
304 broad peak between 9 am–6 pm for biogenic emissions, as the emission rate of isoprene from vegetation is
305 largely depended on ambient temperature and sunlight intensity. Higher levels of diesel and gasoline vehicular
306 emissions were observed in the evening and early morning due to a reduced mixing height and increased
307 emissions from the morning and evening rush hour. Lower concentrations observed during daytime hours were
308 likely due to decreased emissions, increased mixing height and enhanced photochemical loss (Yuan et al., 2009).
309 The diurnal pattern of fuel evaporation was also similar to the vehicular emissions trends, except the amplitude
310 was much weaker, with a difference between maximum and minimum values of ~6 $\mu\text{g}/\text{m}^3$. We identified higher
311 concentrations of industrial emissions at night and in the early morning, with values remaining fairly stable
312 during daytime hours. This finding is consistent with other observations in urban and rural areas (Yuan et al.,
313 2009).



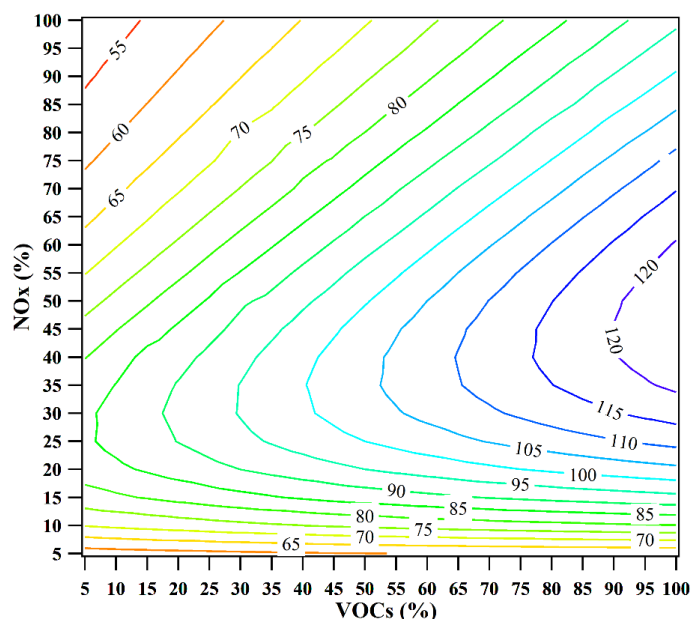
314
315

Figure 5. Diurnal patterns in source concentrations of the five identified sources

316 3.4 Contributions of VOC sources to O₃ formation

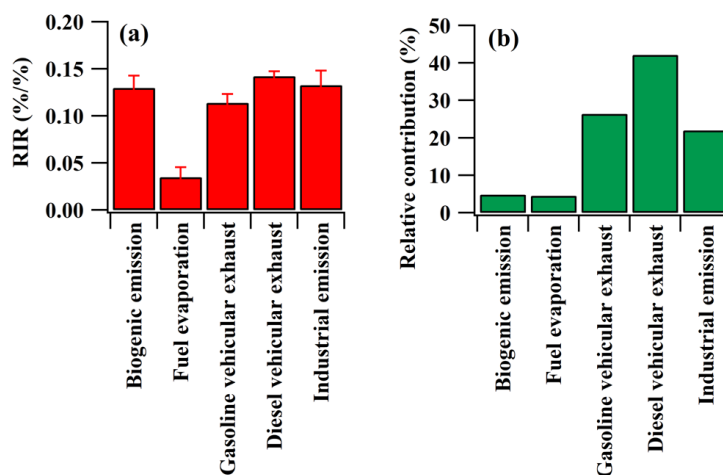
317 To highlight the relative contributions of the different emissions on VOC abundance during the 88 O₃ episode
318 days, we extracted and averaged the contributions of the different sources from the PMF model. We found that
319 the contributions of gasoline vehicular exhausts had significantly increased during O₃ episode days, with a mean
320 average percentage of $41 \pm 5\%$.

321 Figure 6 shows the O₃ isopleth plot illustrating the relationship between VOCs and NO_x concentrations on the
322 O₃ mixing ratio. The plot is the output from the OBM-MCM model, and is based on the mean diurnal variability
323 of observed air pollutants on O₃ episode days. Based on the current scenario (with 100% VOCs and 100% NO_x),
324 the O₃ mixing ratio decreased with the reduction of VOCs and increased with the reduction of NO_x, indicating
325 that O₃ formation in this site is VOC-limited and is consistent with previous results observed in Nanjing (Wang
326 et al., 2009; Zhang et al., 2009; Cai et al., 2010; Kurokawa et al., 2013; Ding et al., 2016). O₃ formation was
327 found to be VOC-limited until NO_x had decreased to a mixing ratio of 45%. Furthermore, O₃ formation becomes
328 NO_x-limited when the NO_x mixing ratios are reduced by > 70%. Overall, the O₃ isopleth results suggest that
329 minimizing VOC emissions would be effective at reducing O₃ formation at the JAES site.



330
331 **Figure 6.** The ozone isopleth in terms of the percentage change of VOCs and NO_x. The ozone mixing ratios are in ppbv.

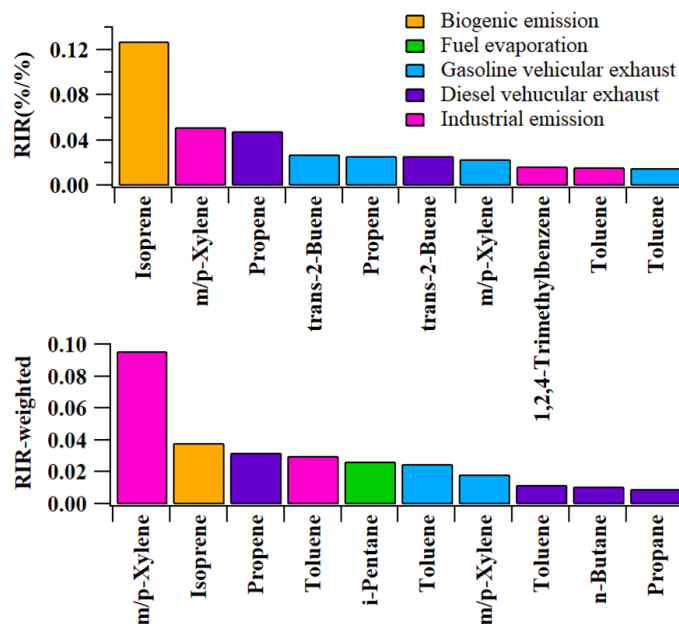
332 To further investigate the formulation and implementation of VOCs and their emissions, we simulated the RIR
333 values of each source for all of the O₃ episode days using the OBM-MCM model (Fig. 7). The RIR value
334 represents the percentage change in O₃ production per percent change in the precursors. Positive RIR values
335 indicate reduced O₃ formation with reduced source concentration, while negative values would indicate the
336 opposite. A larger absolute RIR value indicates a stronger impact of a particular source on O₃ formation. Our
337 results infer positive VOC RIR values and negative NO RIR values (-0.34 ± 0.09), indicating O₃ formation to
338 be VOC-limited, which is consistent with the O₃ isopleth analysis. This observation is also consistent with
339 previous results in industrial, traffic, residential and commercial areas of Nanjing (Zhang et al., 2018; An et al.,
340 2015). However, the RIR values of each source were found to vary day-to-day due to the variability in the mixing
341 ratios of VOCs and NO_x, as well as changes in meteorological parameters. Figure 7a shows the mean RIR values
342 of the different emission sources. Diesel vehicular exhausts were found to have the largest RIR value of $0.14 \pm$
343 0.01 , followed by industrial emissions (0.13 ± 0.02), biogenic emissions (0.12 ± 0.01), gasoline vehicle exhausts
344 (0.11 ± 0.01), and fuel evaporation (0.03 ± 0.01). Therefore, VOC species in diesel vehicular exhausts and
345 industrial emissions had the highest impact on O₃ photochemical formation at the JAES site. Furthermore, we
346 calculated the relative contributions of the different sources based on the reactivity and abundance of individual
347 VOC species. Our results showed that vehicle exhausts were the highest contributors to O₃ formation at ~68%,
348 with diesel and gasoline vehicular exhausts contributing 42% and 26%, respectively. This was followed by
349 industrial emissions (22%), biogenic emissions (5%), and fuel evaporation (5%). Our results further demonstrate
350 the need to minimize VOC emissions from vehicle exhausts in order to lower O₃ formation and photochemical
351 pollution.



352
353 **Figure 7a. The average RIR values of VOC sources, and (b) the relative contributions of different VOC sources to**
354 **photochemical O₃ formation.**

355 To further investigate the relative importance of individual VOC species in each source, we calculated the RIR
356 values and relative contributions of individual VOC species to photochemical O₃ formation. Figure 8 illustrates
357 the 10 VOC species with highest RIR and RIR-weighted values at the JAES site. Based on the mass
358 concentrations of individual species in each source, we found that *m,p*-xylene and toluene in industrial emissions
359 and gasoline vehicular emissions, propene and toluene in diesel vehicular emissions, and *i*-pentane in fuel
360 evaporation to be the dominant species contributing to photochemical formation in each VOC source. Thus, only
361 a small number of VOCs species can be monitored for effective control on local O₃ formation. Though the
362 photochemical reactivity of *i*-pentane, propane and *n*-butane were lower than alkenes and aromatics, their high
363 RIR-weighted values indicate that high concentrations of VOCs with low photochemical reactivity can still
364 significantly contribute towards O₃ formation. This finding further confirms that both VOC reactivity and
365 abundance should be considered for effective control on O₃ formation. Isoprene in biogenic emissions also shows
366 high RIR-weighted values when considering both its reactivity and abundance. Currently, the majority of the
367 VOCs control measures are focused on anthropogenic emissions, yet the contributions of biogenic emissions on
368 O₃ formation are also significant (section 3.5). This feature highlights the need to minimize VOCs from biogenic
369 emissions for effective control on O₃ formation.

370



371
372 **Figure 8.** The average RIR values and RIR-weighted values of the top 10 VOC species in the different source categories.

373 3.5 Policy summary and implications

374 To effectively control photochemical pollution, the Prevention and Control of Atmospheric Pollution Act was
375 passed in 1987 and amended recently in 2015. As a result, a series of measures to prevent and control VOCs
376 levels have been and are being implemented by central and local governments, including the implementation of
377 new laws and regulations, and the advancement of technology. The results of this study suggest that
378 photochemical O₃ formation within the urban areas of Nanjing city are VOC-limited, which is consistent with
379 observations in the urban locations of other regions, including the North China Plain, the Yangtze River Delta
380 and the Pearl River Delta. Minimizing VOC emissions and their concentrations should therefore be prioritized
381 in order to alleviate O₃ pollution. The prevention and control of VOC pollution has been listed as one of the key
382 tasks of “the Blue Sky” Project initiated in 2012 by the Department of Environmental Protection of Jiangsu
383 Province. Furthermore, the administrative measures on the Prevention and Control of Volatile Organic
384 Compounds Pollution in Jiangsu (Order No. 119 of the Provincial Government) was enacted on March 6, 2018
385 and implemented on May 1, 2018, with the aim to control VOC emissions in Jiangsu Province.

386
387 In order to achieve these goals, various measures have been implemented (Table S2), including: 1) investigating
388 the current pollution status and identifying the progress of VOCs prevention and control in Jiangsu Province
389 (Provincial Office of the Joint Conference on the prevention and control of air pollution [2012] No. 2); 2)
390 conducting a strict industry access system, under the Advice on Promoting Air Pollution Joint Prevention and
391 Control Work to Improve Regional Air Quality (Office of the State Council [2010] No. 33); 3) strengthening the
392 remediation on existing sources of VOCs and reducing VOC emissions from these sources, under the Guidelines
393 for the Implementation of Leak Detection and Repair (LDAR) in Jiangsu Province (Trial) (Provincial Office of
394 Environmental Protection [2013] No. 318); 4) strengthening the VOC monitoring capacity, under the Guidelines
395 for Control of Volatile Organic Compounds Pollution in Key Industries in Jiangsu Province (Provincial Office
396 of Environmental Protection [2013] No. 128); 5) improving standards on VOC emissions for key industries,
397 including standards for surface coating of the automobile manufacturing industry (DB32/2862-2016), the
398 chemical industry (DB32/3151-2016), and furniture manufacturing operations (DB32/3152-2016), which are



399 still effective since their enforcement; 6) implementing the Pilot Measures for Volatile Organic Compounds
400 Discharge Charges (Ministry of Finance [2015] No. 71) on October 1, 2015 to raise awareness of emissions
401 reduction in factories and to control VOC emissions from industrial sources; 7) encouraging the public to live a
402 low-carbon life and to supervise and make recommendations in accordance with the laws, under the Measures
403 for Public Participation in Environmental Protection in Jiangsu Province (Trial) (Provincial Regulation of
404 Environmental Protection Office [2016] No. 1).

405
406 Based on the VOC source apportionment results in this study, we identified vehicular emissions and industrial
407 emissions to be the two major VOC sources contributing to photochemical O₃ formation. Other measures and/or
408 regulations have been conducted in the Jiangsu Province to effectively control VOCs emissions from vehicles
409 and industry. For vehicular emissions, the Regulations on Prevention and Control of Vehicle Exhaust Pollution
410 in Nanjing was amended in July 2017, and subsequently in March, 2018
411 (<http://hbt.jiangsu.gov.cn/col/col1590/index.html>). The new regulation not only focusses on vehicle emissions,
412 but also incorporates a number of additional topics, including optimizing the function and distribution of urban
413 areas, limiting the number of vehicles in the region, promoting new green energy vehicles, and improving the
414 quality of fuel. It is advised to promote intelligent traffic management, implement a priority strategy for public
415 transportation, and construct more efficient traffic systems to promote pedestrian and bicycle use. Further studies
416 should be conducted to estimate and manage the increasing quantity of vehicles on the road. As of January 1,
417 2017, these regulations specify that all new and used vehicles should meet the fifth phase of vehicle emission
418 standards, including vehicle manufacturing, selling, registering and importing. For the vehicles already on the
419 road, an environmental protection examination should be monitored annually, based on the standards of GB
420 14622-2016, GB 18176-2016, GB 19755-2016, and HJ 689-2014. Penalties are issued if qualified vehicles
421 excessively emit pollutants due to poor maintenance.

422
423 For industrial emissions, various policies have been implemented to reduce VOC emissions, particularly in
424 chemical industries: including, 1) investigations on the VOC emissions of the chemical industry and the
425 establishment of an archive system for VOC pollution control, particularly the inspection of industry information,
426 products and materials, unorganized emission of storage, and exhaust gas treatment facilities, under the Plan for
427 Investigation of Volatile Organic Pollutant Emissions in Jiangsu Province, mentioned in the Provincial Office of
428 Environmental Protection [2012] No. 183; 2) exhaust gas remediation in the chemical industry park, under the
429 Technical Specifications for Prevention and Control of Air Pollution in Chemical Industries in Jiangsu Province
430 (Provincial Office of Environmental Protection [2014] No. 3), which states the establishment of the long-term
431 supervision of exhaust gas remediation in the chemical industry park of Jiangsu Province; 3) a pilot project on
432 the leak detection and repair (LDAR) technology in the chemical industry park, under the notification on carrying
433 out the technical demonstration and pilot work of leak detection and repair (LDAR) in petrochemical and
434 chemical industries (Provincial Office of Environmental Protection [2015] No. 157). The TVOC removal
435 efficiency of organic exhaust vents should be >95%, and higher for areas of excessive environmental pollution
436 at >97% (GB 31571-2015).

437
438 Overall, though measures have been adopted to improve standards and control vehicle VOCs emissions, most
439 of these policies only focus on total VOC emissions (or the mass of total emissions) and do not consider the
440 impacts of individual VOC species. To accelerate the implementation of existing policies and to strengthen
441 collaborative regional prevention and control, priority should be placed on specific high-impact VOC species
442 (i.e., *m,p*-xylene and toluene in the industrial emission and gasoline vehicular emission) by considering both
443 their reactivity and abundance. It is also necessary to consider the reduction ratios of VOC/NO_x when VOCs and
444 NO_x are simultaneously controlled. Finally, long-term monitoring studies are necessary to determine the cost-
445 benefits and performance of each policy.

446 4. Conclusion

447 In this study, a one-year field sampling campaign was conducted to investigate the VOCs characteristics at an
448 urban site in Nanjing (the JAES site), Jiangsu province. In total, 56 VOCs including 29 alkanes, 10 alkenes, 16



449 aromatics and acetylene were identified and quantified. The composition analysis found that alkanes were the
450 dominant group of VOCs observed at the JAES site (~53%), followed by aromatics, acetylene, and alkenes. This
451 finding is consistent with the VOCs measurements in studies conducted in the North China Plain, Pearl River
452 Delta, and Yangtze River Delta. We observed distinct seasonal patterns of TVOCs, with maximum values in
453 winter and minimum values in summer. Similarly, prominent morning and evening peaks were observed in the
454 diurnal variability of TVOCs, influenced by local emissions and meteorology.

455
456 Based on the observed VOCs data, we identified five dominant VOC sources at the JAES site using a PMF
457 model. By considering both the abundance and reactivity of individual VOC species in each source, the OBM-
458 MCM model identified vehicular and industrial emissions, particularly *m,p*-xylene, toluene and propene, to be
459 the main contributors of O₃ pollution. Our results demonstrate that O₃ formation at the JAES site is VOC-limited
460 and is predominantly controlled by a small number of VOCs species. Local governments have strengthened
461 several measures to minimize VOCs pollution from vehicle and industrial emissions in the Jiangsu province in
462 recent years, though most of these policies focus particularly on lowering the total emissions of VOCs. However,
463 our results highlight the need to consider both the abundance and reactivity of individual VOC species in order
464 to formulate effective control strategies to minimize pollution. Further, despite its low relative contribution to
465 the TVOC, our results identified biogenic emissions to be a stronger source of O₃ formation when considering
466 both VOC species abundance and reactivity. We therefore suggest the implementation of measures to monitor
467 and control both the contributions of biogenic and anthropogenic emissions to effectively minimize O₃ pollution
468 in Nanjing.



469 **Author Contributions.** Qiuyue Zhao and Dr. Liu designed the research and carried them out. Dr. Ling performed the model simulation. Dr. Shen performed
470 the observation data analysis. Qiuyue Zhao prepared the manuscript with contributions from all co-authors.

471 **Competing Interests.** The authors declare that they have no conflict of interest.

472 **Acknowledgements.** This work was supported by National Key R&D Program of China (Nos.2016YFC0207607 and 2017YFC0210106), Open Research
473 Fund of Jiangsu Province Key Laboratory of Environmental Engineering (No. ZX2016002). This work was also partly supported by the National Natural
474 Science Foundation of China (No. 41775114), and the Pearl River Science & Technology Nova Program of Guangzhou (201806010146).

475 **Reference**

476 An, J., Zhu, B., Wang, H., Li, Y., Lin, X., and Yang, H.: Characteristics and source apportionment of VOCs measured in an industrial area of Nanjing,
477 Yangtze River Delta, China, *Atmospheric Environment*, 97, 206-214, 2014

478
479 An, J., Zou, J., Wang, J., Lin, X., and Zhu, B.: Differences in ozone photochemical characteristics between the megacity Nanjing and its suburban
480 surroundings, Yangtze River Delta, China, *Environmental Science and Pollution Research International*, 22(24), 19607, 2015.

481
482 Cai, C. J., Geng, F. H., Tie, X.X., and An, J. L.: Characteristic and source apportionment of VOCs measured in Shanghai, China, *Atmospheric Environment*,
483 44, 5005-5014, 2010.

484
485 Cardelino, C. A., and Chameides W. L.: An observation-based model for analyzing ozone precursor relationships in the urban atmosphere, *Air and Waste
486 Management Association*, 45, 161-180, 1995.

487
488 Carter, W.L., and Atkinson, R.: Computer modeling study of incremental hydrocarbon reactivity, *Environmental Science and Technology* 23, 864-880,
489 1989.

490
491 Ding, A.J., Nie, W., Huang, X., Chi, X.G., Xu, Z., et al.: Ozone in the western Yangtze River Delta of China: a synthesis study based on ground, aircraft
492 and sounding measurement 2011-2015, The 6th PEEEX meeting, May 2016, 2016

493
494 Fu, L., Wan, W., Zhang, W., and Cheng, H.: Air pollution prevention and control progress in Chinese cities, *Clean Air Asia, China*, available at:
495 <http://cleanairasia.org/wp-content/uploads/2016/08/China-Air-2016-Report-Full.pdf>, 2016, last access: 16 May 2018.

496
497 Guo, H., Cheng, H. R., Ling, Z. H., Louie, P. K. K., and Ayoko, G. A.: Which emission sources are responsible for the volatile organic compounds in the



- 498 atmosphere of Pearl River Delta?, *Journal of Hazardous Materials*, 188, 116-124, 2011a.
499
500 Guo, H., Zou, S. C., Tsai, W. Y., Chan, L. Y., and Blake, D. R.: Emission characteristics of non-methane hydrocarbons from private cars and taxis at different
501 driving speeds in Hong Kong, *Atmos. Environ.*, 45, 2711–2721, 2011b
502
503 Guo, H., Zheng J. Y., Characterisation of VOC sources and integrated photochemical ozone analysis in Hong Kong and the Pearl River Delta region. Report
504 to the Environmental Protection Department of Hong Kong (Tender Reference AS12-02909), Department of Civil and Environmental Engineering, The
505 Hong Kong Polytechnic University, 2016.
506
507 He, Z., Wang, X., Ling, Z., Zhao, J., Guo, H., Shao, M., and Wang, Z.: Contributions of different anthropogenic volatile organic compound sources to ozone
508 formation at a receptor site in the Pearl River Delta region and its policy implications, *Atmos. Chem. Phys.*, 19, 8801–8816, 2019.
509
510 HKEPD (Hong Kong Environmental Protection Department): Characterisation of VOC sources and integrated photochemical ozone analysis in Hong Kong
511 and the Pearl River Delta region. Final report, , Hong Kong, 2015.
512
513 Huang, C., Chen, C. H., Li, L., Cheng, Z., Wang, H. L., Huang, H. Y., Streets, D. G., Wang, Y. J., Zhang, G. F., and Chen, Y. R.: Emission inventory of
514 anthropogenic air pollutants and VOC species in the Yangtze River Delta region, China. *Atmos. Chem. Phys.*, 11, 4105–4120, 2011a
515
516 Jenkin, M. E. and Clemitshaw, K. C.: Ozone and other secondary photochemical pollutants: chemical processes governing their formation in the planetary
517 boundary layer, *Atmospheric Environment*, 34, 2499–2527, 2000.
518
519 Kurokawa, J., Ohara, T., Morikawa, T., Hanayama, S., Janssens-Maenhout, G., Fukui, T., Kawashima, K., and Akimoto, H.: Emissions of air pollutants
520 and greenhouse gases over Asia regions during 2000–2008: Regional Emission inventory in Asia (REAS) version 2, *Atmos. Chem. Phys.*, 13, 11019–11058,
521 2013.
522
523 Lam, S. H. M., Saunders, S. M., Guo, H., Ling, Z. H., Jiang, F., Wang, X. M., and Wang, T. J.: Modelling VOC source impacts on high ozone episode days
524 observed at a mountain summit in Hong Kong under the influence of mountain-valley breezes. *Atmos. Environ.*, 81, 166–176, 2013
525
526 Lau, A. K. H., Yuan, Z., Yu, J. Z., and Louie, P. K.: Source apportionment of ambient volatile organic compounds in Hong Kong, *Science of the Total
527 Environment*, 408, 4138–4149, 2010.
528
529 Li, X., Rohrer, F., Brauers, T., Hofzumahaus, A., and Wahner, A.: Modeling of HCHO and CHOCHO at a semi-rural site in southern China during the
530 PRIDE-PRD 2006 campaign, *Atmos. Chem. Phys.*, 14, 33013–33054, 2014.
531
532 Ling, Z. H., and Guo, H.: Contribution of VOC sources to photochemical ozone formation and its control policy implication in Hong Kong, *Environmental
533 Science and Policy*, 38(3), 180–191, 2014.
534
535 Ling, Z. H., Guo, H., Cheng, H. R., and Yu, Y. F.: Sources of ambient volatile organic compounds and their contributions to photochemical ozone formation



- 536 at a site in the Pearl River Delta, southern China, *Environmental Pollution*, 159, 2310-2319, 2011.
537
- 538 Liu, B., Liang, D., Yang, J., Dai, Q., Bi, X., and Feng, Y., Yuan, J., Xiao, Z.M., Zhang, Y.F., Xu, H.: Characterization and source apportionment of volatile
539 organic compounds based on 1-year of observational data in Tianjin, China. *Environmental Pollution*, 218, 757-769 2015.
540
- 541 Liu, Y., Shao, M., Fu, L. L., Lu, S. H., Zeng, L. M., and Tang, D. G.: Source profiles of volatile organic compounds (VOCs) measured in China: Part I,
542 *Atmospheric Environment* 42, 6247-6260, 2008a.
543
- 544 Liu, Y., Shao, M., Lu, S., Chang, C. C., Wang, J. L., and Fu, L.: Source apportionment of ambient volatile organic compounds in the Pearl River delta,
545 China: part II, *Atmospheric Environment*, 42(25), 6261-6274, 2008b.
546
- 547 Liu, Y., Shao, M., Lu, S., Chang, C., Wang, J. L., and Chen, G.: Volatile organic compound (VOC) measurements in the Pearl River delta (PRD) region,
548 China, *Atmos. Chem. Phys.*, 7(5), 1531-1545, 2008c.
549
- 550 Lyu, X., Chen, N., Guo, H., Zhang, W., Wang, N., Wang, Y., and Liu, M.: Ambient volatile organic compounds and their effect on ozone production in
551 Wuhan, central China, *Science of the Total Environment*, 548-549(60), 483-483, 2016.
552
- 553 Mo, Z., Shao, M., and Lu, S.: Compilation of a source profile database for hydrocarbon and OVOC emissions in China, *Atmospheric Environment*, 143,
554 209-217, 2016.
555
- 556 Mo, Z., Shao, M., Lu, S., Qu, H., Zhou, M., and Gou, B.: Process-specific emission characteristics of volatile organic compounds (VOCs) from
557 petrochemical facilities in the Yangtze River Delta, China, *Science of the Total Environment*, 533, 422-431, 2015.
558
- 559 Mo, Z., Shao, M., Lu, S. H., Niu, H., Zhou, M. Y., Sun, J.: Characterization of non-methane hydrocarbons and their sources in an industrialized coastal city,
560 Yangtze River Delta, China, *Science of the Total Environment*, 593-594, 641-653, 2017.
561
- 562 Ou, J., Guo, H., Zheng, J., Cheung, K., Louie, P. K. K., Ling, Z., and Wang D. W.: Concentrations and sources of non-methane hydrocarbons (NMHCs)
563 from 2005 to 2013 in Hong Kong: a multi-year real-time data analysis, *Atmospheric Environment*, 103(103), 196-206, 2015.
564
- 565 Pan, X., Kanaya, Y., Tanimoto, H., Inomata, S., Wang, Z., Kudo, S., and Uno, I.: Examining the major contributors of ozone pollution in a rural area of the
566 Yangtze River Delta region during harvest season, *Atmos. Chem. Phys.*, 15, 6101-6111, 2015
567
- 568 Saunders, S. M., Jenkin, M. E., Derwent, R. G., and Pilling, M. J.: Protocol for the development of the Master Chemical Mechanism, MCM v3 (Part A):
569 tropospheric degradation of nonaromatic volatile organic compounds, *Atmos. Chem. Phys.*, 3, 161-180, 2003.
570
- 571 Seinfeld, J. H. and Pandis, S. N.: *Atmospheric Chemistry and Physics: from air pollution to climate change*, 2nd edition. Wiley Publisher, New Jersey, USA,
572 2006.
573



- 574 Shao, M., Lu, S., Liu, Y., Xie, X., Chang, C., Huang, S., and Chen, Z.: Volatile organic compounds measured in summer in Beijing and their role in ground-
575 level ozone formation, *Journal of Geophysical Research*, 114, D00G06, doi: 10.1029/2008JD010863, 2009.
576
- 577 Shao, P., An, J. L., Xin, J. Y., Wu, F. K., Wang, J. X., Ji, D. S., and Wang, Y.S.: Source apportionment of VOCs and the contribution to photochemical ozone
578 formation during summer in the typical area in the Yangtze River Delta, China, *Atmospheric Research*, 176-177, 64-74, 2016.
579
- 580 Song, Y., Dai, W., Shao, M., Liu, Y., Lu, S. H., Kuster, W, and Goldan, P.: Comparison of receptor models for source apportionment of volatile organic
581 compounds in Beijing, China, *Environmental Pollution*, 156, 174-183, 2008.
582
- 583 Statistical yearbook of Nanjing. Nanjing Statistic Bureau: <http://221.226.86.104/file/nj2004/2014/jiaotongyunshu/index.htm>, last access: 17 May 2018,
584 2014
585
- 586 Sun, J. J., Li, Z. Y., Xue, L. K., Wang, T., Wang, X. F., Gao, J., Nie, W., Simpson, I.J., Gao, R., Blake, D. R., Chai, F. H., and Wang, W.X.: Summertime
587 C1-C5 alkyl nitrates over Beijing, northern China: spatial distribution, regional transport, and formation mechanisms, *Atmospheric Research*, 204, 102-
588 109. 2018.
589
- 590 Volkamer, R., San Martini, F., Molina, L. T., Salcedo, D., Jimenez, J. L., and Molina, M. J.: A missing sink for gas-phase glyoxal in Mexico City: Formation
591 of secondary organic aerosol, *Geophysical Research Letters*, 34, 255-268, 2007.
592
- 593 Wang, H., Chen, C., Wang, Q., Huang, C., Su, L., Huang, H., Lou, S., Zhou, M., Li, L., Qiao, L., and Wang, Y.: Chemical loss of volatile organic compounds
594 and its impact on the source analysis through a two-year continuous measurement, *Atmospheric Environment*, 80, 488-498, 2013.
595
- 596 Wang, H. L., Lou, S. R., Huang, C., Qiao, L. P., Tang, X. B., Chen, C. H., Zeng, L. M., Wang, Q., Zhou, M., Lu, S. H., and Yu, X.N.: Source profiles of
597 volatile organic compounds from biomass burning in Yangtze River Delta, China, *Aerosol and Air Quality Research*, 14, 818-828, 2014
598
- 599 Wang, M., Shao, M., Chen, W., Lu, S., Liu, Y., Yuan, B., and Li, Y.: Trends of non-methane hydrocarbons (NMHCs) emissions in Beijing during 2002-
600 2013, *Atmos. Chem. Phys.*, 15, 1489-1502, 2015.
601
- 602 Wang, T., Wei, X. L., Ding, A. J., Poon, C. N., Lam, K. S., Li, Y. S., Chan, L. Y., and Anson, M.: Increasing surface ozone concentrations in the background
603 atmosphere of Southern China, 1994–2007, *Atmos. Chem. Phys.*, 9, 6217-6227, 2009.
604
- 605 Wang, Y., Wang, H., Guo, H., Lyu, X., Cheng, H., Ling, Z., Louie P., Simpson, I., Meinardi, S., Blake, D., : Long-term O₃-precursor relationships in Hong
606 Kong: field observation and model simulation, *Atmos. Chem. Physics.*, 17(18), 1-29, 2017.
607
- 608 Xia, L., Cai, C., Zhu, B., An, J., Li, Y., and Li, Y.: Source apportionment of VOCs in a suburb of Nanjing, China, in autumn and winter, *Journal of*
609 *Atmospheric Chemistry*, 71(3), 175-193, 2014a.
610
- 611 Xia, S., Zhao, Q., Li, B., and Shen, G.: Anthropogenic source VOCs emission inventory of Jiangsu Province (In Chinese), *Research of Environmental*



- 612 Sciences, 27(2), 120-126, 2014b.
613
614 Xu, Z. N., Huang, X., Nie, W., Chi, X. G., Xu, Z., Zheng, L. F., Sun, P., Ding, and A. J.: Influence of synoptic condition and holiday effects on VOCs and
615 ozone production in the Yangtze River Delta region, China, *Atmospheric Environment*, 168, 112-124, 2017.
616
617 Xue, L., Wang, T., Louie, P. K., Luk, C. W., Blake, D. R., Xu, Z.: Increasing external effects negate local efforts to control ozone air pollution: a case study
618 of Hong Kong and implications for other Chinese cities, *Environmental Science and Technology*, 48(18), 10769, 2014.
619
620 Yuan, B., Chen, W.T., Shao, M., Wang, M., Lu, S.H., Wang, B., Liu, Y., Chang, C.C., Wang, B: Measurements of ambient hydrocarbons and carbonyls in
621 the Pearl River Delta (PRD), China, *Atmos. Res.*, 116, 93-104, 2012.
622
623 Yuan, Z., Lau, A. K. H., Shao, M., Louie, P. K. K., Liu, S. C., and Zhu, T.: Source analysis of volatile organic compounds by positive matrix factorization
624 in urban and rural environments in Beijing, *Journal of Geophysical Research*, 114, D00G15, doi:10.1029/2008JD011190, 2009.
625
626 Zhang, J., Wang, Y., Wu, F., Lin, H., and Wang, W.: Nonmethane hydrocarbon measurements at a suburban site in Changsha City, China. *Sci. Total Environ.*,
627 408 (2), 312-317, 2009.
628
629 Zhang, X., Xue, Z., Li, H., Yan, L., Yang, Y., Wang, Y., Duan, J., Li, L., Chai, F., Cheng, M., Zhang, W.: Ambient volatile organic compounds pollution in
630 China, *Journal of Environmental Sciences*, 55, 69-75, 2017.
631
632 Zhang, Y. X., An, J. L., Wang, J. X., Shi, Y. Z., Liu, J. D., and Liang, J. S.: Source analysis of volatile organic compounds in the Nanjing industrial area and
633 evaluation of their contribution to ozone, *Environmental Science*, 39(2), 502-510, 2018.
634
635 Zhang, Y. L., Wang, X. M., Barletta, B., Simpson, I.J., Blake, D.R., Fu, X.X., Zhang, Z., He Q.F., Liu, T.Y., Zhao, X.Y., Ding, X.: Source attributions of
636 hazardous aromatic hydrocarbons in urban, suburban and rural areas in the Pearl River Delta (PRD) region, *Journal of Hazardous Materials*, 250-251, 403-
637 411, 2013.
638
639 Zhao, Q, Shen, G., Li, L., Chen, F., Qiao, Y.Z., Li C.Y., Liu Q., and Han, J.Z.: Ambient Particles (PM₁₀, PM_{2.5}, and PM_{1.0}) and PM_{2.5} chemical components
640 in Western Yangtze River Delta (YRD): An Overview of Data from 1-year Online Continuous Monitoring at Nanjing, *Aerosol Science and Engineering*, 1,
641 107-118, 2017.
642
643 Zheng, J. Y., Shao, M., Che, W. W., Zhang, L. J., Zhong, L. J., Zhang, Y. H., and Streets, D.: Speciated VOC emission inventory and spatial patterns of
644 ozone formation potential in the Pearl River Delta, China, *Environ. Sci. Technol.*, 43, 8580-8586, 2009.
645
646 Zhou, D., Li, B., Huang X., Virkkula, A., Wu, H.S., Zhao, Q.Y., Zhang, J., Liu, Q., Li, L., Li, C.Y., Chen, F., Yuan, S.Y., Qiao, Y.Z., Shen, G.F., and Ding
647 A.J.: The impacts of emission control and regional transport on PM_{2.5} ions and carbon components in Nanjing during the 2014 Nanjing Youth Olympic
648 Games, *Aerosol and Air Quality Research*, 17(3), 730-740, 2017.
649



650 Zou, Y., Deng, X. J., Zhu, D., Gong, D. C., Wang, H., Li, F., Tan, H. B., Deng, T., Mai, B. R., Liu, X. T., and Wang, B. G.: Characteristics of 1 year of
651 observational data of VOCs, NO_x and O₃ at a suburban site in Guangzhou, China, Atmos. Chem. Phys., 15, 6625–6636, 2015.
652